Consistency relation for R^p inflation

Hayato Motohashi
Kavli Institute for Cosmological Physics, The University of Chicago, Chicago, Illinois 60637, U.S.A.
(Dated: April 20, 2015)

We consider R^p inflation with $p \approx 2$, allowing small deviation from R^2 inflation. Using the inflaton potential in the Einstein frame, we construct a consistency relation between the scalar spectral index, the tensor-to-scalar ratio, as well as the running of the scalar spectral index, which will be useful to constrain a deviation from R^2 inflation in future observations.

arXiv:1411.2972v2 [astro-ph.CO] 17 Apr 2015

I. INTRODUCTION

The first self-consistent model of inflation is R^2 inflation proposed by Starobinsky in 1980 [1], where R is the Ricci curvature. This model incorporates a graceful exit to the radiation-dominated stage via a period of reheating, where the standard model particles are created through the oscillatory decay of the inflaton, or dubbed the scalaron [2–4]. The predictions of R^2 inflation for the spectra of primordial density perturbations and gravitational waves remain in agreement with the most recent high-precision data of the cosmic microwave background (CMB) [5, 6]. In March 2014, BICEP2 announced the detection of B-mode polarization at degree angular scales in the CMB, and the amplitude of the tensor-to-scalar-ratio is as large as $r = 0.20^{+0.07}_{-0.05}$ [7], which is in tension with previous data as well as the prediction of R^2 inflation. However, it is still unclear if the signal is of primordial origin, due to an unknown amplitude of foreground dust emission [8]. In light of this, R^2 inflation is still consistent with the recent data and upcoming data may allow us to pin down the inflationary model of our universe.

In addition to inflation, the R^2 term play a different role in the context of $f(R)$ gravity for the late-time acceleration. By choosing a suitable functional form of $f(R)$, $f(R)$ gravity can mimic the expansion history of the concordance ΛCDM model without a cosmological constant [9–11]. Observationally, a key to distinguish $f(R)$ gravity from the ΛCDM model is the expansion history and the growth of the large-scale structure, which are conveniently parametrized by the equation-of-state parameter w for dark energy and the growth index γ, respectively, because both parameters remain constant in the ΛCDM model, namely, $w = -1$ and $\gamma = 0.55$, while they are dynamical in $f(R)$ gravity [9, 12–17]. In particular, it is interesting that $f(R)$ gravity allows a 1 eV sterile neutrino [18], whose existence has been suggested by recent neutrino oscillation experiments but is in tension with vanilla ΛCDM. However, the $f(R)$ models for the late-time acceleration suffer from singularity problems, where the scalaron mass and Ricci curvature diverge quickly in the past [11, 19–22]. These problems are solved if we add R^2 term [23]. The resultant combined $f(R)$ model incorporates inflation and the late-time acceleration. In the combined model, inflationary dynamics is still the same as R^2 inflation, while differences show up in reheating phase dominated by the kinetic energy of the scalaron [24], which enhances the tensor power spectrum [25].

The R^2 model is thus attractive in the sense that it is currently one of the leading candidates for inflation and it cures singularity problems when combined with $f(R)$ models for the late-time acceleration. Although it is simple and powerful, with progress in observational accuracy, we can test for further complexity. Similar to the generalization from a scale-invariant spectrum to a nonzero tilt, we may be forced to consider a small deviation from R^2 inflation. Specifically, tiny tensor-to-scalar ratio for R^2 inflation, namely, $r \simeq 0.003$ for 60 e-folds, motivates us to consider a deviation from R^2 inflation. We are poised to possibly obtain strong constraints on r from joint analysis of Planck and BICEP2 data, along with future experiments. It is therefore interesting to consider the possibility to generate larger value of r based on the R^2 model.

In order to establish a way to measure a deviation from R^2 inflation, we investigate R^p inflation in the present paper, where $p \approx 2$ and is not an integer, allowing small deviation from $p = 2$. The R^p Lagrangian was originally considered in the context of higher derivative theories [26, 27] and then applied to inflation [28, 29] (see also [30–32] for recent review), which provides a simple and economical generalization of R^2 inflation. Recently, R^p inflation has been focused in the context of the generation of large r. It has been emphasized that for p slightly smaller than 2, the tensor-to-scalar ratio can be enhanced relative to the original R^2 model [33] (see also [34]). A combined $f(R)$ model based on the R^p model has also been proposed [35]. Not only is it of phenomenological interest, the R^p action is also theoretically motivated because one-loop corrections to the R^2 action could give a correction to the power of the Ricci scalar [33, 36, 37]. A deformation of the R^2 action that mimics higher-loop corrections is considered in [38]. A relevance to Higgs inflation is considered in [39, 40].

However, its prediction to the scalar spectral index n_s, the tensor-to-scalar ratio r, as well as the running of the scalar spectral index $\alpha \equiv dn_s/d\ln k$ is not well formulated. In particular, some of the previous results provide different results for the prediction of n_s and r. Further, the running of the scalar spectral index in the model has not been discussed in the literature. The aim of the present paper is to resolve these issues and present a consistency relation

for R^p inflation by using the inflaton potential in the Einstein frame. We consider not only the scalar spectral index and the tensor-to-scalar ratio, but also the running of the scalar spectral index. We derive a handy expression for these inflationary observables, which will be useful to constrain a deviation from R^2 inflation in future observations.

The organization of the paper is as follows. In Sec. II, we explore the background dynamics of the inflationary expansion in R^p inflation. We write down the inflaton potential for general p in the Einstein frame and the slow-roll parameters in terms of the derivatives of the potential. In Sec. III, we derive a consistency relation between the inflationary observables, with which we can constrain the model. We conclude in Sec. IV. Throughout the paper, we will work in natural units where $c = 1$, and the metric signature is $(-+++)$.

II. R^p INFLATION

Let us start with a general $f(R)$ and write down equations of motion in the Einstein frame. We consider

$$S = \int d^4x\sqrt{-g}\frac{M_{\rm Pl}^2}{2}f(R), \tag{1}$$

where $M_{\rm Pl} \equiv (8\pi G)^{-1/2}$ is the reduced Planck mass. By using the conformal transformation $g^E_{\mu\nu} \equiv F(R)g_{\mu\nu}$ with defining the scalaron field ϕ by $F(R) \equiv f'(R) \equiv e^{\sqrt{\frac{2}{3}}\frac{\phi}{M_{\rm Pl}}}$, we can recast the action as

$$S = \int d^4x\sqrt{-g_E}\left[\frac{M_{\rm Pl}^2}{2}R_E - \frac{1}{2}g_E^{\mu\nu}\partial_\mu\phi\partial_\nu\phi - V(\phi)\right], \tag{2}$$

where the potential is given by

$$V(\phi) = \frac{M_{\rm Pl}^2}{2}\frac{\chi F(\chi) - f(\chi)}{F(\chi)^2}. \tag{3}$$

Here, $\chi = \chi(\phi)$ is a solution for $F(\chi) = e^{\sqrt{\frac{2}{3}}\frac{\phi}{M_{\rm Pl}}}$, and thus $f(\chi)$ and $F(\chi)$ are determined for each ϕ. The time and the scale factor in the Jordan frame and Einstein frame relate through

$$dt_E = \sqrt{F}dt, \quad a_E = \sqrt{F}a, \tag{4}$$

and thus the Hubble parameter in the Einstein frame is given by

$$H_E = \frac{H}{\sqrt{F}}\left(1 + \frac{\dot{F}}{2HF}\right), \tag{5}$$

where a dot implies the derivative with respect to the time t in the Jordan frame. The Einstein equation reads

$$3M_{\rm Pl}^2H_E^2 = \frac{1}{2}\left(\frac{d\phi}{dt_E}\right)^2 + V, \tag{6}$$

$$-2M_{\rm Pl}^2\frac{dH_E}{dt_E} = \left(\frac{d\phi}{dt_E}\right)^2, \tag{7}$$

and the equation of motion for the scalaron is given by

$$\frac{d^2\phi}{dt_E^2} + 3H_E\frac{d\phi}{dt_E} + V_\phi = 0, \tag{8}$$

where $V_\phi \equiv \partial V/\partial\phi$.

For the rest of the paper, we focus on the following model:

$$f(R) = R + \lambda R^p. \tag{9}$$

The parameter p is not necessarily an integer in general, and λ has mass dimension $(2-p)$. In this model, the potential (3) can be explicitly written in terms of ϕ as

$$V(\phi) = V_0e^{-2\sqrt{\frac{2}{3}}\frac{\phi}{M_{\rm Pl}}}\left(e^{\sqrt{\frac{2}{3}}\frac{\phi}{M_{\rm Pl}}} - 1\right)^{\frac{p}{p-1}} \tag{10}$$

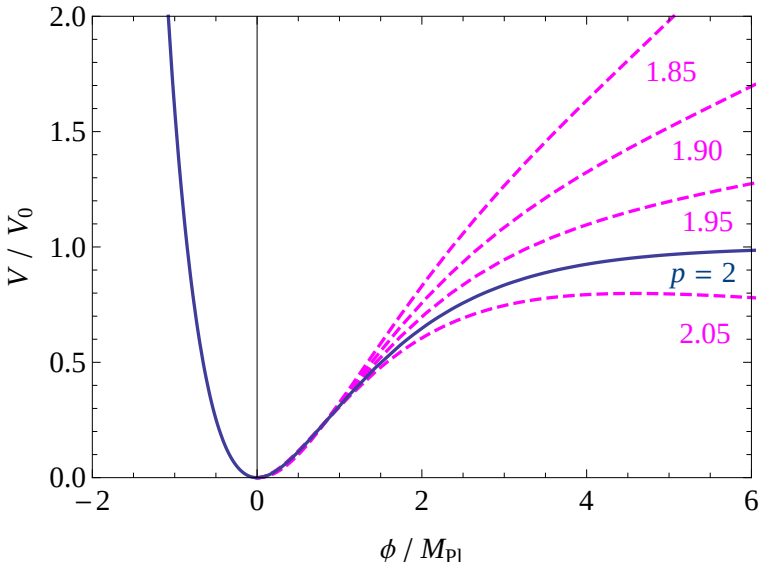

Figure 1. Potential for R^p inflation with $p = 2$ (blue solid), and 1.85, 1.90, 1.95, 2.05 (magenta dashed).

with $V_0 \equiv \frac{M_{\rm Pl}^2}{2}(p-1)p^{p/(1-p)}\lambda^{1/(1-p)}$. Note that for $p = 2$ and $\lambda = 1/(6M^2)$, the potential (10) recovers the potential for R^2 inflation:

$$V(\phi) = \frac{3}{4}M^2 M_{\rm Pl}^2(1 - e^{-\sqrt{\frac{2}{3}}\frac{\phi}{M_{\rm Pl}}})^2, \tag{11}$$

where the energy scale is normalized as $M \simeq 10^{13}$ GeV from the amplitude of observed power spectrum for the primordial perturbations.

In Fig. 1, we present the potential (10) for various p around $p = 2$. The scalaron rolls slowly on the potential at $\phi > 0$, and leads the inflationary expansion. While the potential for $p = 2$ asymptotically approaches to a constant value V_0 for large ϕ, the potential for $p \lesssim 2$ continuously grows. Therefore, the potential for $p \lesssim 2$ is steeper than $p = 2$, and this leads to larger tensor-to-scalar ratio relative to R^2 inflation, as we shall see later. For $p > 2$, the potential (10) has a maximum at $\phi = M_{\rm Pl}\sqrt{\frac{3}{2}}\ln\left[\frac{2(p-1)}{p-2}\right] \equiv \phi_m$ and approaches to 0 for large ϕ. For instance, $\phi_m/M_{\rm Pl} \simeq 4.58$ for $p = 2.05$. Therefore, inflation can take place at either of $0 < \phi < \phi_m$ or $\phi > \phi_m$. We are interested in the former case to see a deviation from R^2 inflation, and do not consider the latter case, which leads to a completely different scenario from R^2 inflation.

We define the slow-roll parameters for the potential in the Einstein frame as

$$\epsilon \equiv \frac{M_{\rm Pl}^2}{2}\left(\frac{V_\phi}{V}\right)^2, \quad \eta \equiv M_{\rm Pl}^2\frac{V_{\phi\phi}}{V}, \quad \xi \equiv M_{\rm Pl}^4\frac{V_\phi V_{\phi\phi\phi}}{V^2}. \tag{12}$$

Under the slow roll approximation, (6) – (8) read

$$H_E \simeq \frac{\sqrt{V}}{\sqrt{3}M_{\rm Pl}}, \quad \frac{dH_E}{dt_E} \simeq -\frac{V_\phi^2}{6V}, \quad \frac{d\phi}{dt_E} \simeq -\frac{M_{\rm Pl}V_\phi}{\sqrt{3V}}. \tag{13}$$

During slow-roll regime, the scale factor in the Einstein frame undergoes a quasi-de Sitter expansion. From $|\dot{F}/(HF)| \simeq 2\sqrt{\epsilon/3} \ll 1$, F remains approximately constant during the slow-roll regime. Hence, from (4) the scale factor and time in the Einstein frame are identical to those in the Jordan frame up to a constant factor. Consequently, the quasi-de Sitter expansion takes place in both frame. The number of e-folds between an initial time t_{Ei} and t_E is given by

$$N_E \equiv \int_{t_{Ei}}^{t_E} H_E dt_E \simeq \frac{1}{M_{\rm Pl}^2}\int_\phi^{\phi_i}\frac{V}{V_\phi}d\phi. \tag{14}$$

Note that from (4) and (5) $H_E dt_E = H dt[1 + \dot{F}/(2HF)] \simeq H dt$ during the slow-roll regime and therefore $N_E \simeq N$. Armed with these equivalences between quantities in the Jordan frame and Einstein frame during inflation, we omit the subscript E for the following and continue to explore the inflationary dynamics in the Einstein frame.

Before proceeding to detailed analysis for $p = 2$ and general p, let us here clarify the differences of the potential in the previous works. In [39], the authors consider R^p model (9) at first but eventually investigate the potential $V \propto (1 - \gamma e^{-\beta\phi})$ with β and γ as free parameters. This potential is obviously different from the potential (10) in R^p inflation because their potential approaches constant for large ϕ. They show that $\epsilon \ll |\eta|$ always holds, and n_s depends only on e-folds while r depends on the model parameters and e-folds. As we shall see below, these points are incompatible with R^p inflation.

In [40], the authors also start from R^p model (9) but arrive the potential $V \propto e^{\frac{2-p}{p-1}\sqrt{\frac{2}{3}}\frac{\phi}{M_{\rm Pl}}}$, assuming $\phi/M_{\rm Pl} \gg \sqrt{3/2} \simeq 1.22$. However, as we shall see, a field value which we are interested in is the same order of 1.22. In particular, their approximation breaks down as $p \to 2$, because the field value of our interest becomes closer to 1.22. Actually, their n_s and r does not recover R^2 inflation. Therefore, we cannot use their result if we want to consider small deviation from R^2 inflation.

Thus, although both works are motivated by R^p inflation, they did not investigate R^p inflation itself. Rather, they investigated the potential $V \propto (1 - \gamma e^{-\beta\phi})$ and $V \propto e^{\frac{2-p}{p-1}\sqrt{\frac{2}{3}}\frac{\phi}{M_{\rm Pl}}}$, respectively, both of which cannot be used as an asymptotic form of the potential (10) of R^p inflation. On the other hand, our analysis is based on the potential (10) without any approximation.

A. $p = 2$

First, let us focus on the case with $p = 2$. The slow-roll parameters (12) for the potential (11) are given by

$$\begin{aligned}
\epsilon &= \frac{4}{3(e^{\sqrt{\frac{2}{3}}\frac{\phi}{M_{\rm Pl}}} - 1)^2}, \\
\eta &= -\frac{4(e^{\sqrt{\frac{2}{3}}\frac{\phi}{M_{\rm Pl}}} - 2)}{3(e^{\sqrt{\frac{2}{3}}\frac{\phi}{M_{\rm Pl}}} - 1)^2}, \\
\xi &= \frac{16(e^{\sqrt{\frac{2}{3}}\frac{\phi}{M_{\rm Pl}}} - 4)}{9(e^{\sqrt{\frac{2}{3}}\frac{\phi}{M_{\rm Pl}}} - 1)^3}.
\end{aligned} \tag{15}$$

Thus the slow-roll parameters relate each other through ϕ, and we can derive the following relation between them:

$$\begin{aligned}
\eta &= -\frac{2\sqrt{\epsilon}}{\sqrt{3}} + \epsilon, \\
\xi &= \frac{4}{3}\epsilon - 2\sqrt{3}\epsilon^{3/2}.
\end{aligned} \tag{16}$$

Note that these relations are derived by only using the form of the potential. They hold exactly, regardless of the appearance of the slow-roll parameters. As we shall see later, it is when we convert these relations into a consistency relation between inflationary observables that we need the slow-roll approximation.

For $\phi > M_{\rm Pl}$, the slow roll parameters are suppressed as ϵ, $\xi \sim e^{-2\sqrt{\frac{2}{3}}\frac{\phi}{M_{\rm Pl}}}$, and $|\eta| \sim e^{-\sqrt{\frac{2}{3}}\frac{\phi}{M_{\rm Pl}}}$. It is worthwhile to note that the hierarchy between the slow-roll parameters is not $1 \gg \epsilon \sim |\eta| \gg \xi$ like ϕ^2 inflation, but $1 \gg |\eta| \gg \epsilon \sim \xi$, which leads to a tiny tensor-to-scalar ratio.

If we define the end of inflation by $\epsilon = 1$, a field value at the end of inflation ϕ_f is given by $\phi_f/M_{\rm Pl} \simeq 0.940$. From (14), we obtain the e-folds between ϕ_i and ϕ as

$$N(\phi) = \frac{3}{4}\left(e^{\sqrt{\frac{2}{3}}\frac{\phi_i}{M_{\rm Pl}}} - e^{\sqrt{\frac{2}{3}}\frac{\phi}{M_{\rm Pl}}}\right), \tag{17}$$

where we neglect a linear term of $(\phi - \phi_i)$, which gives a few percent correction. We can solve this equation for ϕ,

$$\frac{\phi(N)}{M_{\rm Pl}} = \sqrt{\frac{3}{2}}\ln\left(e^{\sqrt{\frac{2}{3}}\frac{\phi_i}{M_{\rm Pl}}} - \frac{4}{3}N\right), \tag{18}$$

and using the slow-roll equation (13) with the potential (11), the Hubble parameter is given by

$$\frac{H(N)}{\sqrt{V_0}/M_{\rm Pl}} = \frac{1}{\sqrt{3}}\left[1 - \left(e^{\sqrt{\frac{2}{3}}\frac{\phi_i}{M_{\rm Pl}}} - \frac{4}{3}N\right)^{-1}\right], \tag{19}$$

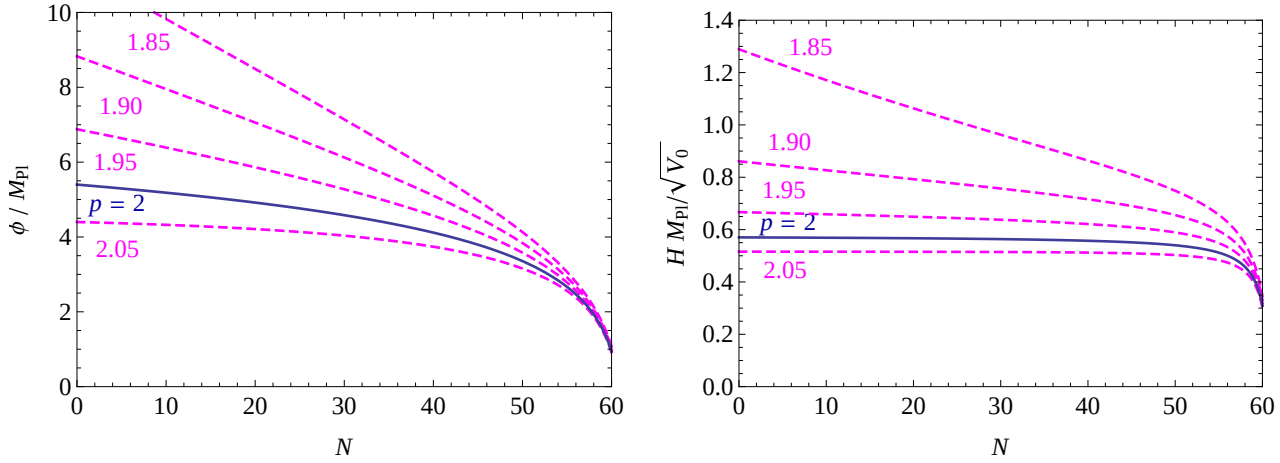

Figure 2. Time evolution of the scalaron ϕ and the Hubble parameter H for $p = 2$ (blue solid), and 1.85, 1.90, 1.95, 2.05 (magenta dashed).

which are presented as a blue solid line in Fig. 2.

If we require the total e-folds $N_k \equiv N(\phi_f) = 60$, we obtain $\phi_i/M_{\rm Pl} \simeq 5.40$. Therefore, $N_k \simeq \frac{3}{4}e^{\sqrt{\frac{2}{3}}\frac{\phi_i}{M_{\rm Pl}}}$, and at the leading order of N_k, the slow roll parameters (15) at $\phi \simeq \phi_i$ are expressed as

$$\epsilon = \frac{3}{4N_k^2}, \quad \eta = -\frac{1}{N_k}, \quad \xi = \frac{1}{N_k^2}. \tag{20}$$

B. $p \approx 2$

We proceed to a general case with $p \approx 2$. The slow-roll parameters (12) are given by

$$\begin{aligned}
\epsilon &= \frac{[(2-p)F + 2(p-1)]^2}{3(p-1)^2(F-1)^2}, \\
\eta &= \frac{2[(2-p)^2F^2 - (p-1)(5p-8)F + 4(p-1)^2]}{3(p-1)^2(F-1)^2}, \\
\xi &= \frac{4[(2-p)F + 2(p-1)][(2-p)^3F^3 + (p-1)(2p-3)(5p-8)F^2 - (p-1)^2(17p-24)F + 8(p-1)^3]}{9(p-1)^4(F-1)^4},
\end{aligned} \tag{21}$$

where $F \equiv e^{\sqrt{\frac{2}{3}}\frac{\phi}{M_{\rm Pl}}}$ as we defined the above. We can confirm that For $p = 2$, (21) reproduces (15). We can erase F from these equations and obtain

$$\begin{aligned}
&-4(2-p) + 2(3p-4)\sqrt{3\epsilon} - 6\epsilon + 3p\eta = 0, \\
&-2(2-p)(3p-4)\sqrt{3\epsilon} + 3(7p^2 - 24p + 24)\epsilon - 9\sqrt{3}(3p-4)\epsilon^{3/2} + 9(2-p)\epsilon^2 - \frac{9}{4}p^2\xi = 0.
\end{aligned} \tag{22}$$

Again, these relations hold without the slow-roll approximation.

The field value at the end of inflation $\epsilon = 1$ is given by

$$\frac{\phi_f}{M_{\rm Pl}} = \sqrt{\frac{3}{2}} \ln \left[\frac{(2+\sqrt{3})(p-1)}{(1+\sqrt{3})p - (2+\sqrt{3})} \right]. \tag{23}$$

For instance, $\phi_f/M_{\rm Pl} \simeq 0.907, 0.978, 1.02, 1.07$ for $p = 2.05, 1.95, 1.90, 1.85$, respectively.

The number of e-folds between ϕ_i and ϕ given by (14) reads

$$N(\phi) = \frac{3p}{4(2-p)} \ln \left[\frac{(2-p)e^{\sqrt{\frac{2}{3}}\frac{\phi_i}{M_{\rm Pl}}} + 2(p-1)}{(2-p)e^{\sqrt{\frac{2}{3}}\frac{\phi}{M_{\rm Pl}}} + 2(p-1)} \right]. \tag{24}$$

Then we obtain

$$\frac{\phi(N)}{M_{\rm Pl}} = \sqrt{\frac{3}{2}} \ln\left[E^{-1}\left(e^{\sqrt{\frac{2}{3}}\frac{\phi_i}{M_{\rm Pl}}} + \frac{2(p-1)}{2-p}\right) - \frac{2(p-1)}{2-p}\right]. \tag{25}$$

From (13), the Hubble parameter is given by

$$\frac{H(N)}{\sqrt{V_0}/M_{\rm Pl}} = \frac{1}{\sqrt{3}}\left[E^{-1}\left(e^{\sqrt{\frac{2}{3}}\frac{\phi_i}{M_{\rm Pl}}} + \frac{2(p-1)}{2-p}\right) - \frac{p}{2-p}\right]^{\frac{p}{2(p-1)}}\left[E^{-1}\left(e^{\sqrt{\frac{2}{3}}\frac{\phi_i}{M_{\rm Pl}}} + \frac{2(p-1)}{2-p}\right) - \frac{2(p-1)}{2-p}\right]^{-1}, \tag{26}$$

where $E(N) \equiv e^{4(2-p)N/(3p)}$. We present the time evolution of the scalaron and the Hubble parameter for $p = 2.05$, 1.95, 1.90, 1.85 by magenta dashed lines in Fig. 2. As expected, the scalaron rolls down faster for $p \lesssim 2$.

By setting $N_k \equiv N(\phi_f) = 60$, we obtain

$$\frac{\phi_i}{M_{\rm Pl}} = \sqrt{\frac{3}{2}} \ln\left[E_k\left(e^{\sqrt{\frac{2}{3}}\frac{\phi_f}{M_{\rm Pl}}} + \frac{2(p-1)}{2-p}\right) - \frac{2(p-1)}{2-p}\right], \tag{27}$$

where $E_k \equiv e^{4(2-p)N_k/(3p)}$. For instance, $\phi_i/M_{\rm Pl} \simeq 4.40$, 6.88, 8.83, 11.2 for $p = 2.05$, 1.95, 1.90, 1.85, respectively. Therefore, for N_k we can neglect the contribution from ϕ_f and end up with

$$N_k \simeq \frac{3p}{4(2-p)} \ln\left[\frac{(2-p)}{2(p-1)} e^{\sqrt{\frac{2}{3}}\frac{\phi_i}{M_{\rm Pl}}} + 1\right]. \tag{28}$$

By taking the limit of $p \to 2$, we recover $N_k = \frac{3}{4} e^{\sqrt{\frac{2}{3}}\frac{\phi_i}{M_{\rm Pl}}}$.

By substituting $F = 2(E_k - 1)(p-1)/(2-p)$, we obtain the slow-roll parameters (21) at $\phi \simeq \phi_i$ as

$$\begin{aligned}
\epsilon &= \frac{4E_k^2(2-p)^2}{3[2(p-1)E_k - p]^2}, \\
\eta &= \frac{4(2-p)[2(2-p)E_k^2 - pE_k + p]}{3[2(p-1)E_k - p]^2}, \\
\xi &= \frac{16E_k(2-p)^2[4(2-p)^2E_k^3 + 2p(4p-7)E_k^2 - p(11p-18)E_k + p(3p-4)]}{9[2(p-1)E_k - p]^4}.
\end{aligned} \tag{29}$$

Taking the limit $p \to 2$, we can recover the results in R^2 inflation.

In R^2 inflation, the hierarchy between the slow-roll parameters is $|\eta| \gg \epsilon \sim \xi$. However, it is not the case for R^p inflation with $p \neq 2$. The left panel of Fig. 3 exhibits the slow roll parameters (29) for $p \approx 2$ with $N_k = 60$ and 50. Blue solid, magenta dashed, and green dot-dashed lines are ϵ, $|\eta|$, and ξ, respectively. Thick lines are for $N_k = 60$, while thin lines are for $N_k = 50$. Note that η flips its sign at $p \simeq 1.94$ for $N_k = 60$ ($p \simeq 1.93$ for $N = 50$): $\eta > 0$ for $p \lesssim 1.94$, and $\eta < 0$ for $p \gtrsim 1.94$. Now the hierarchy between the slow-roll parameters for $p \approx 2$ obviously varies from $|\eta| \gg \epsilon \sim \xi$ for $p = 2$. However, we note that ξ is always subleading. Therefore, for the following, we treat ϵ and η as the first order quantities, and ξ as the second order quantity.

III. CONSISTENCY RELATION

Now we want to relate the slow-roll parameters to the inflationary observables. Since the comoving curvature perturbation and the tensor perturbation are invariant under the conformal transformation [41, 42], we can make use of the slow-roll parameters obtained from the inflaton potential in the Einstein frame to evaluate the scalar spectral index n_s, its running $\alpha \equiv dn_s/d\ln k$, and the tensor-to-scalar ratio r. Up to the leading order of the slow-roll parameters, the inflationary observables can be written as

$$\begin{aligned}
n_s - 1 &= -6\epsilon + 2\eta, \\
r &= 16\epsilon, \\
\alpha &= 16\epsilon\eta - 24\epsilon^2 - 2\xi.
\end{aligned} \tag{30}$$

Let us remind that ξ is treated as the second order quantity here. This treatment is valid for R^p inflation and is also often implicitly assumed in the literature, but it is not necessarily always the case. For general case, where ξ can be comparable to ϵ and $|\eta|$, we need more careful treatment [43].

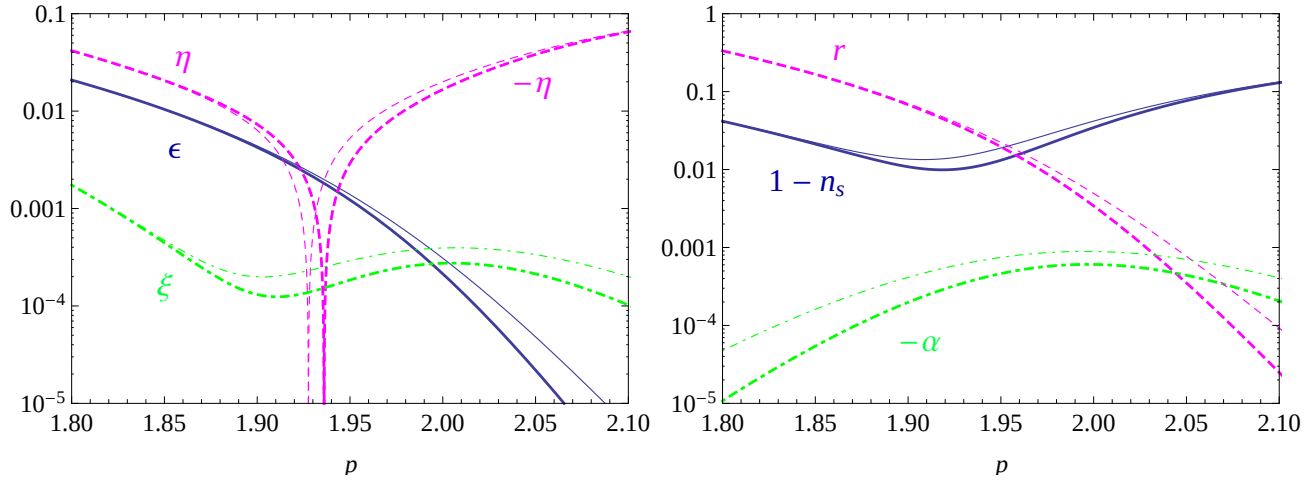

Figure 3. Left: Slow roll parameters, ϵ (blue solid), $|\eta|$ (magenta dashed), and ξ (green dot-dashed). Right: Inflationary observables, $1-n_s$ (blue solid), r (magenta dashed), and $-\alpha$ (green dot-dashed). The thick lines and thin lines are for $N_k = 60$ and 50, respectively.

A. $p = 2$

For $p = 2$, we can immediately write down (30) in terms of N_k by the virtue of (20). Up to the leading order of N_k^{-1}, we obtain

$$n_s - 1 = -\frac{2}{N_k}, \quad r = \frac{12}{N_k^2}, \quad \alpha = -\frac{2}{N_k^2}. \tag{31}$$

Thus the consistency relation is given by

$$n_s - 1 = -\sqrt{\frac{r}{3}}, \quad \alpha = -\frac{r}{6}. \tag{32}$$

Equivalently, we can derive the above relation using (16) and (30).

B. $p \approx 2$

For general p, by substituting (29) into (30), we obtain

$$\begin{aligned} n_s - 1 &= -\frac{8(2-p)[(2-p)E_k^2 + p(E_k - 1)]}{3[2(p-1)E_k - p]^2}, \\ r &= \frac{64E_k^2(2-p)^2}{3[2(p-1)E_k - p]^2}, \\ \alpha &= -\frac{32p(2-p)^2E_k(E_k-1)(2E_k - 3p + 4)}{9[2(p-1)E_k - p]^4}. \end{aligned} \tag{33}$$

Thus, n_s, r, and α are related through the parameter $E_k = e^{4(2-p)N_k/(3p)}$. We can recover (31) if we take the limit $p \to 2$ in (33). By erasing E_k, we can obtain the consistency relation as

$$\begin{aligned} n_s - 1 &= -\frac{(3p-4)}{\sqrt{3}p}\sqrt{r} - \frac{3p-2}{8p}r + \frac{8(2-p)}{3p}, \\ \alpha &= \frac{4(2-p)(3p-4)}{3\sqrt{3}p^2}\sqrt{r} - \frac{15p^2 - 40p + 24}{6p^2}r - \frac{(3p-4)(4p-3)}{8\sqrt{3}p^2}r^{3/2} - \frac{(p-1)(3p-2)}{32p^2}r^2. \end{aligned} \tag{34}$$

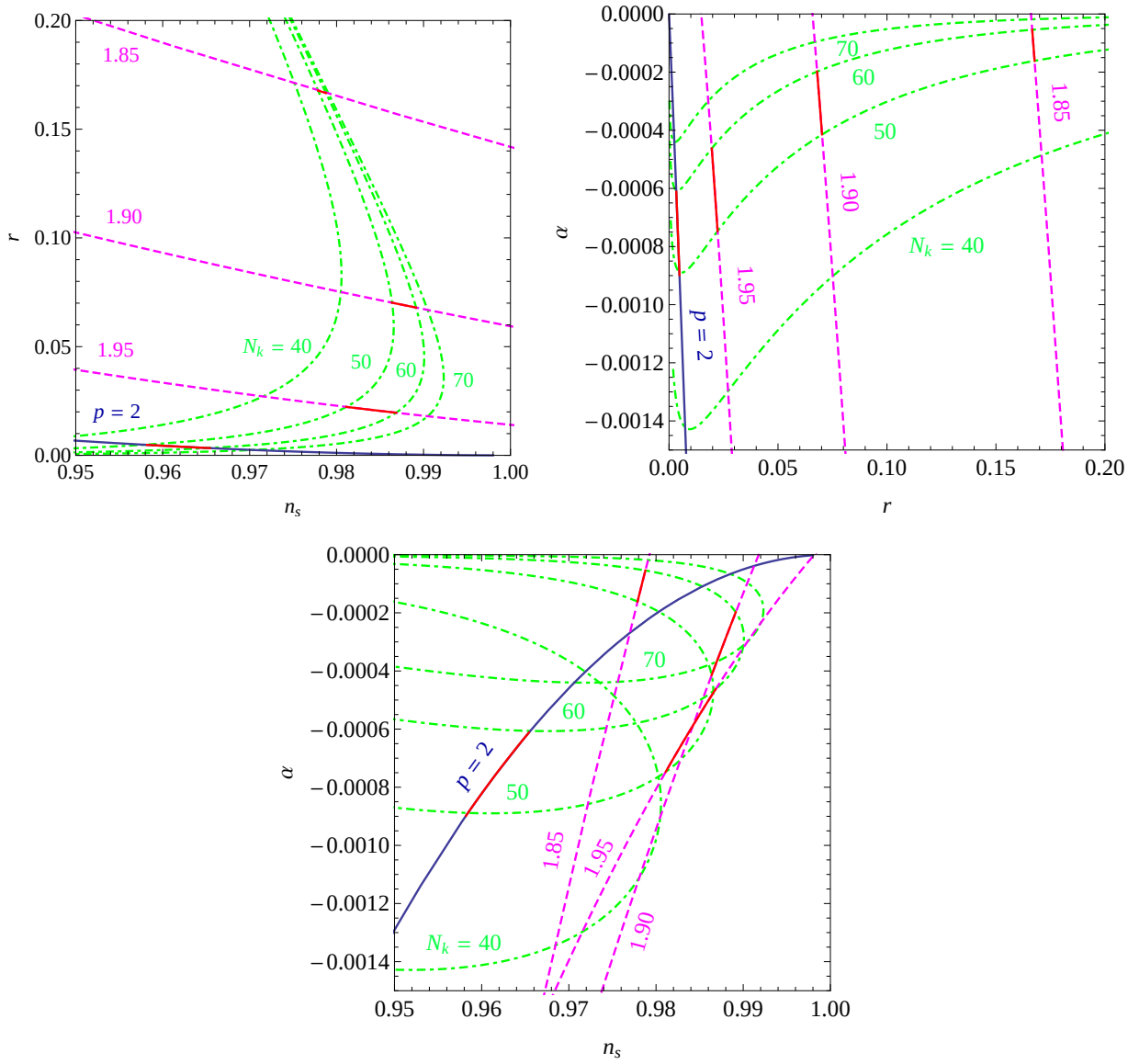

Figure 4. Scalar spectral index n_s, its running α, and tensor-to-scalar ratio r for $p = 2$ (solid blue), and 1.95, 1.90, 1.85 (magenta dashed), where e-folds between $N_k = 50$ and 60 are highlighted (red solid). Lines for fixed e-folds $N_k = 40$, 50, 60, 70 (green dot-dashed) are also shown.

In the right panel of Fig. 3, we present the scalar spectral index, its running, and the tensor-to-scalar ratio for $p \approx 2$ with $N_k = 60$ and 50. Blue solid, magenta dashed, green dot-dashed lines are $(1 - n_s)$, r, $-\alpha$, respectively, and thick and thin lines represent $N_k = 60$ and 50, respectively. We see that the scalar spectral index takes its maximum value $\simeq 0.99$ at $p \simeq 1.92$ and thus R^p inflation describe only red-tilted spectrum. For $p < 1.8$ or $p > 2$, we have $n_s < 0.96$. On the other hand, the tensor-to-scalar ratio increases as p decreases. Actually, r exceeds 0.1 and 0.2 at $p \simeq 1.88$ and $p \simeq 1.84$, respectively, for $N_k = 60$. As for the running of the scalar spectral index, α is always negative. Its amplitude takes the maximum value $\simeq 10^{-3}$ at $p \simeq 2$.

Using (33) or (34), we can explicitly draw the consistency relation between the inflationary observables as presented in Fig. 4. Blue solid lines represent $p = 2$, and magenta dashed lines represent $p = 1.95$, 1.90, 1.85. We also show lines for fixed e-folds N_k by green dot-dashed lines. We highlighted lines for fixed p with e-folds $50 < N_k < 60$. In particular, it is interesting that the scalar spectral index n_s is sensitive for a deviation from $p = 2$. The panel for (n_s, r) captures this property. For $1.8 < p < 2$, the spectral index varies as $0.96 \lesssim n_s \lesssim 0.99$ but is always larger than 0.96 for $N_k = 60$. For $p \gtrsim 1.95$, the spectral index is very sensitive for p. Therefore, the parameter region $p \gtrsim 1.95$ is solely constrained by n_s.

We are also interested in how future constraint on r tests the model. From the panel for (n_s, r) in Fig. 4, we note that for $N_k = 60$ small tensor-to-scalar ratio with $r \leq 0.05$ requires $1.92 \lesssim p \leq 2$ and $0.96 \lesssim n_s \lesssim 0.99$. For large r with $0.05 \leq r \leq 0.1$, p should be $1.88 \lesssim p \lesssim 1.92$ and n_s needs to be within $0.98 \lesssim n_s \lesssim 0.99$. On the other hand, for fixed $n_s = 0.96$, $r = 0.05$ and 0.1 require $(p, N_k) \simeq (1.93, 30)$ and $(1.9, 27)$, respectively.

From the panel for (r, α) in Fig. 4, we can explicitly see that a deviation from $p = 2$ suppresses α, while r is enhanced. This property is also useful to test R^p inflation. We can constrain p with an order 10^{-4} accuracy for α. The panel for (n_s, α) in Fig. 4 shows that it is difficult for this combination is to constrain p because the lines are overlapping and thus there is a degeneracy between parameters. Therefore, in order to constrain R^p inflation, it is important to measure both the scalar and the tensor spectra, namely, the combination of (n_s, r) or (r, α) would constrain the model significantly.

IV. CONCLUSIONS

We investigated R^p inflation with $p \approx 2$ in order to evaluate deviations from R^2 inflation. Using the inflaton potential in the Einstein frame, we explicitly wrote down the scalar spectral index n_s, its running α, and the tensor-to-scalar ratio r as in (33), which are presented in Fig. 3. We can also explicitly draw the consistency relation as presented in Fig. 4. We showed that the parameter region $p \gtrsim 1.95$ is solely constrained by n_s and a precise measurement of (n_s, r) or (r, α) can test a whole range of p. Specifically, for $N_k = 60$, $r \leq 0.05$ requires $1.92 \lesssim p \leq 2$ and $0.96 \lesssim n_s \lesssim 0.99$, while $0.05 \leq r \leq 0.1$ requires $1.88 \lesssim p \lesssim 1.92$ and $0.98 \lesssim n_s \lesssim 0.99$. On the other hand, for fixed $n_s = 0.96$, $r \simeq 0.05$ and 0.1 require $(p, N_k) \simeq (1.93, 30)$ and $(1.9, 27)$, respectively.

ACKNOWLEDGMENTS

We thank W. Hu and and A. A. Starobinsky for useful discussions. This work was supported by Japan Society for the Promotion of Science Postdoctoral Fellowships for Research Abroad.

[1] A. A. Starobinsky, Phys.Lett. **B91**, 99 (1980).
[2] A. Vilenkin, Phys.Rev. **D32**, 2511 (1985).
[3] M. B. Mijic, M. S. Morris, and W.-M. Suen, Phys.Rev. **D34**, 2934 (1986).
[4] L. Ford, Phys.Rev. **D35**, 2955 (1987).
[5] G. Hinshaw *et al.* (WMAP), Astrophys.J.Suppl. **208**, 19 (2013), arXiv:1212.5226 [astro-ph.CO].
[6] P. Ade *et al.* (Planck Collaboration), (2013), arXiv:1303.5082 [astro-ph.CO].
[7] P. Ade *et al.* (BICEP2 Collaboration), Phys.Rev.Lett. **112**, 241101 (2014), arXiv:1403.3985 [astro-ph.CO].
[8] R. Adam *et al.* (Planck Collaboration), (2014), arXiv:1409.5738 [astro-ph.CO].
[9] W. Hu and I. Sawicki, Phys.Rev. **D76**, 064004 (2007), arXiv:0705.1158 [astro-ph].
[10] S. A. Appleby and R. A. Battye, Phys.Lett. **B654**, 7 (2007), arXiv:0705.3199 [astro-ph].
[11] A. A. Starobinsky, JETP Lett. **86**, 157 (2007), arXiv:0706.2041 [astro-ph].
[12] H. Motohashi, A. A. Starobinsky, and J. Yokoyama, Prog.Theor.Phys. **123**, 887 (2010), arXiv:1002.1141 [astro-ph.CO].
[13] H. Motohashi, A. A. Starobinsky, and J. Yokoyama, JCAP **1106**, 006 (2011), arXiv:1101.0744 [astro-ph.CO].
[14] R. Gannouji, B. Moraes, and D. Polarski, JCAP **0902**, 034 (2009), arXiv:0809.3374 [astro-ph].
[15] H. Motohashi, A. A. Starobinsky, and J. Yokoyama, Int.J.Mod.Phys. **D18**, 1731 (2009), arXiv:0905.0730 [astro-ph.CO].
[16] S. Tsujikawa, R. Gannouji, B. Moraes, and D. Polarski, Phys.Rev. **D80**, 084044 (2009), arXiv:0908.2669 [astro-ph.CO].
[17] H. Motohashi, A. A. Starobinsky, and J. Yokoyama, Prog.Theor.Phys. **124**, 541 (2010), arXiv:1005.1171 [astro-ph.CO].
[18] H. Motohashi, A. A. Starobinsky, and J. Yokoyama, Phys.Rev.Lett. **110**, 121302 (2013), arXiv:1203.6828 [astro-ph.CO].
[19] S. Tsujikawa, Phys.Rev. **D77**, 023507 (2008), arXiv:0709.1391 [astro-ph].
[20] S. Appleby and R. Battye, JCAP **0805**, 019 (2008), arXiv:0803.1081 [astro-ph].
[21] A. V. Frolov, Phys.Rev.Lett. **101**, 061103 (2008), arXiv:0803.2500 [astro-ph].
[22] T. Kobayashi and K.-i. Maeda, Phys.Rev. **D78**, 064019 (2008), arXiv:0807.2503 [astro-ph].
[23] S. A. Appleby, R. A. Battye, and A. A. Starobinsky, JCAP **1006**, 005 (2010), arXiv:0909.1737 [astro-ph.CO].
[24] H. Motohashi and A. Nishizawa, Phys.Rev. **D86**, 083514 (2012), arXiv:1204.1472 [astro-ph.CO].
[25] A. Nishizawa and H. Motohashi, Phys.Rev. **D89**, 063541 (2014), arXiv:1401.1023 [astro-ph.CO].
[26] H. Schmidt, Class.Quant.Grav. **6**, 557 (1989).
[27] K.-i. Maeda, Phys.Rev. **D39**, 3159 (1989).
[28] V. Muller, H. Schmidt, and A. A. Starobinsky, Class.Quant.Grav. **7**, 1163 (1990).
[29] S. Gottlober, V. Muller, H. Schmidt, and A. A. Starobinsky, Int.J.Mod.Phys. **D1**, 257 (1992).
[30] A. De Felice and S. Tsujikawa, Living Rev.Rel. **13**, 3 (2010), arXiv:1002.4928 [gr-qc].

[31] J. Martin, C. Ringeval, and V. Vennin, Phys.Dark Univ. (2014), 10.1016/j.dark.2014.01.003, arXiv:1303.3787 [astro-ph.CO].
[32] J. Martin, C. Ringeval, R. Trotta, and V. Vennin, JCAP **1403**, 039 (2014), arXiv:1312.3529 [astro-ph.CO].
[33] A. Codello, J. Joergensen, F. Sannino, and O. Svendsen, JHEP **1502**, 050 (2015), arXiv:1404.3558 [hep-ph].
[34] J. Martin, C. Ringeval, R. Trotta, and V. Vennin, Phys.Rev. **D90**, 063501 (2014), arXiv:1405.7272 [astro-ph.CO].
[35] M. Artymowski and Z. Lalak, JCAP **1409**, 036 (2014), arXiv:1405.7818 [hep-th].
[36] I. Ben-Dayan, S. Jing, M. Torabian, A. Westphal, and L. Zarate, JCAP **1409**, 005 (2014), arXiv:1404.7349 [hep-th].
[37] M. Rinaldi, G. Cognola, L. Vanzo, and S. Zerbini, JCAP **1408**, 015 (2014), arXiv:1406.1096 [gr-qc].
[38] M. Rinaldi, G. Cognola, L. Vanzo, and S. Zerbini, (2014), arXiv:1410.0631 [gr-qc].
[39] R. Costa and H. Nastase, JHEP **1406**, 145 (2014), arXiv:1403.7157 [hep-th].
[40] G. K. Chakravarty and S. Mohanty, (2014), arXiv:1405.1321 [hep-ph].
[41] T. Chiba and M. Yamaguchi, JCAP **0810**, 021 (2008), arXiv:0807.4965 [astro-ph].
[42] J.-O. Gong, J.-c. Hwang, W.-I. Park, M. Sasaki, and Y.-S. Song, JCAP **1109**, 023 (2011), arXiv:1107.1840 [gr-qc].
[43] H. Motohashi and W. Hu, (2015), arXiv:1503.04810 [astro-ph.CO].